Mol Neurobiol (2015) 52:478–491
DOI 10.1007/s12035-014-8848-9

Activation of VEGF/Flk-1-ERK Pathway Induced Blood–Brain Barrier Injury After Microwave Exposure

Li-Feng Wang · Xiang Li · Ya-Bing Gao · Shui-Ming Wang · Li Zhao · Ji Dong · Bin-Wei Yao · Xin-Ping Xu · Gong-Min Chang · Hong-Mei Zhou · Xiang-Jun Hu · Rui-Yun Peng

Received: 27 April 2014 / Accepted: 31 July 2014 / Published online: 9 September 2014

Abstract Microwaves have been suggested to induce neuronal injury and increase permeability of the blood–brain barrier (BBB), but the mechanism remains unknown. The role of the vascular endothelial growth factor (VEGF)/Flk-1-Raf/MAPK kinase (MEK)/extracellular-regulated protein kinase (ERK) pathway in structural and functional injury of the blood–brain barrier (BBB) following microwave exposure was examined. An in vitro BBB model composed of the ECV304 cell line and primary rat cerebral astrocytes was exposed to microwave radiation (50 mW/cm^2, 5 min). The structure was observed by scanning electron microscopy (SEM) and the permeability was assessed by measuring transendothelial electrical resistance (TEER) and horseradish peroxidase (HRP) transmission. Activity and expression of VEGF/Flk-1-ERK pathway components and occludin also were examined. Our results showed that microwave radiation caused intercellular tight junctions to broaden and fracture with decreased TEER values and increased HRP permeability. After microwave exposure, activation of the VEGF/Flk-1-ERK pathway and Tyr phosphorylation of occludin were observed, along with down-regulated expression and interaction of occludin with zonula occludens-1 (ZO-1). After Flk-1 (SU5416) and MEK1/2 (U0126) inhibitors were used, the structure and function of the BBB were recovered. The increase in expression of ERK signal transduction molecules was muted, while the expression and the activity of occludin were accelerated, as well as the interactions of occludin with p-ERK and ZO-1 following microwave radiation. Thus, microwave radiation may induce BBB damage by activating the VEGF/Flk-1-ERK pathway, enhancing Tyr phosphorylation of occludin, while partially inhibiting expression and interaction of occludin with ZO-1.

Keywords Microwave · In vitro blood–brain barrier model · VEGF · ERK · Occludin

Abbreviations

BBB	Blood–brain barrier
EMP	Electromagnetic pulse
ERK	Extracellular-regulated protein kinase
GFAP	Glial fibrillary acidic protein
HRP	Horseradish peroxidase
IM	Inverted microscope
LSCM	Laser scanning confocal microscope
MEK	MAPK kinase
MMP	Matrix metalloproteinase
qRT-PCR	Quantitative real-time PCR
SEM	Scanning electron microscope
TEER	Transendothelial electrical resistance
TJs	Tight junctions
ZO	Zonula occludens

Introduction

Exposure to microwave radiation, a non-ionizing electromagnetic radiation present in the environment, is perceived as a

Li-Feng Wang and Xiang Li are co-first authors.

L.-F. Wang · Y.-B. Gao · S.-M. Wang · L. Zhao · J. Dong · B.-W. Yao · X.-P. Xu · G.-M. Chang · X.-J. Hu (✉) · R.-Y. Peng (✉)
Laboratory of Experimental Pathology, Beijing Institute of Radiation Medicine, 27 Taiping Road, Beijing 100850, China
e-mail: xjhu2003@vip.sina.com
e-mail: pengry12@163.com

X. Li
Human Resource Department, Beijing Chuiyangliu Hospital, 2 Chuiyangliu South Street, Beijing 100022, China

H.-M. Zhou
Radiation Protection, Beijing Institute of Radiation Medicine, 27 Taiping Road, Beijing 100850, China

health risk factor that may cause a variety of adverse effects, such as headaches, sleep disturbances, and even brain tumors [1–3]. However, the mechanism underlying brain damage following microwave radiation remains largely unknown. The blood–brain barrier (BBB) is a selective barrier formed by brain capillary endothelial cells, together with the closely associated astrocytic endfeet processes, perivascular neurons, and pericytes. The BBB restricts entry of substances from the systemic circulation by specialized tight junctions (TJs) between adjacent cells [4]. TJs in these cells are formed by the interaction of specialized cytoskeletal and bridge proteins including specific types of occludins, claudins, zonula occludens (ZO), and junctional adhesion molecules [5]. The BBB permeability is modulated by the cellular localization, expression, and protein–protein interaction of the TJ proteins [6, 7]. Several studies have shown that occludin may be involved in signal transduction and thus is considered as an important component of the BBB [8, 9].

The roles of vascular endothelial growth factors (VEGFs) in the central nervous system are dually dependent on the different physiological and pathological states. VEGF is the key regulator of permeability which may contribute to the disruption of the BBB and facilitate the progression of secondary brain damage [10–12]. The role of VEGF via Flk-1 is carried out by the phosphoinositide 3-kinase(PI3K)/Akt and the MAPK kinase (MEK)/extracellular-regulated protein kinase (ERK) pathways [13, 14]. It is reported that the MAPK-signaling pathway modulates the TJ paracellular transport by up- or down-regulating the expression of several TJ proteins and hence altering the molecular composition within the TJ complexes [15]. ERKs are members of the MAPK and the Raf/MEK/ERK cascade. The ERK1/2 MAPK pathway plays an important role in changing the composition of TJs and altering the permeability of TJ barrier in the brain [16, 17].

Microwaves have been suggested to induce neuronal injury and increase permeability of the BBB [18–21], in which the TJ proteins including occludin, ZO-1, and claudin are abnormally expressed, but the mechanism remains unknown. In this study, an in vitro model was established to observe the changes of BBB permeability and the expression and activity of VEGF/Flk-1, Raf/MEK/ERK, and occludin following microwave radiation. Inhibitors of Flk-1 (SU5416) and MEK1/2 (U0126) were also used to examine the role of VEGF or ERK on the expression and activity of occludin in the injury of BBB permeability induced by microwave radiation.

Materials and Methods

Ethics Statement

All animal work was conducted according to relevant national and international guidelines. The study protocol was approved by the Beijing Institute of Radiation Medicine Animal Care and Use Committee. It was carried out in accordance with the National Institute of Health Guide for the Care and Use of Laboratory Animals.

Cell Culture Preparation

The ECV304 cell line and primary rat cerebral astrocytes were used in a co-culture model to study the BBB in vitro. The ECV304 cell culture medium consisted of Dulbecco's Modified Eagle Medium (DMEM), supplemented with 10 % heat-inactivated fetal calf serum (FCS), 1 % combined penicillin and streptomycin (5,000 U/5,000 mg/ml), and 1 % amphotericin (250 mg/ml). The culture medium was changed every 48 h, and the cells were split 1:20 once a week. The immunostaining of the VIII factor was detected to confirm the endothelial characteristic of the ECV304 cells.

Cerebral cells mainly including neurons and astrocytes were isolated from neonatal rats and seeded into cell culture flasks at a density of $1 \times 10^5/cm^3$ in DMEM medium (Gibco), containing 20 % FBS, L-glutamine (2 M), penicillin (100 IU/ml), and streptomycin (100 IU/ml). The cells were cultured at 37 °C in a humidified atmosphere of 5 % CO_2/95 % air. Pure astrocytes were obtained by sequential passage. The culture medium was changed every 2 days until the cells reached 80 % confluency. Flasks with confluent culture were incubated at 37 °C for 22 h with gentle agitation in a constant temperature shaker at 220 r/min. The medium was refreshed to remove the non-adherent oligodendrocytes and microglia. The purity of astrocytes was identified by immunostaining of GFAP (Boster Biological Technology, Ltd.). In the co-culture model, ECV304 cells and primary astrocytes were cultured in the obverse and reverse of the Snapwell cell culture inserts.

For transendothelial electrical resistance (TEER) measurements, ECV304 and cerebral astrocytes were co-cultured using rat-tail collagen (Sigma)-coated Snapwell cell culture inserts (membrane pore size 0.4 mm, growth surface area 1.1 cm^2; Corning). The ECV304 cells were seeded on the upper side of the collagen-coated insert. After the ECV304 cells reached sub-confluence (70 %), cerebral astrocytes were placed under the insert on the bottom of the well. After 2–3 days in co-culture, the cells were used for the experiments. SU5416 (Flk-1 inhibitor, MERCK, 20 μmol/l) or U0126 (MEK1/2 inhibitor, Cell Signal, 10 μmol/l) was added to the medium at 30 min before radiation to determine the role of VEGF and ERK on the expression and activity of occludin.

Experimental Groups and Microwave Exposure Procedure

The co-culture model and ECV304 cells were placed in 12-well culture plates. Cells from the exposed group were subjected to microwaves for 5 min with a mean power density of 50 mW/cm^2 at a frequency of 2.856 GHz. Microwave energy was transmitted by rectangular waveguide and A16-dB standard-gain horn antenna to an electromagnetic shield chamber (7 m×6.5 m×4 m). The average power densities were measured using a wave guide antenna, the GX12M1CHP power meter (Guanghua Microelectronics Instruments), and GX12M30A power heads. The microwave pulses were delivered at 500 pps, respectively, with a pulse width of 500 ns. The peak field power density tested with a calibrated detector and an oscilloscope for the exposed group was 200 W/cm^2. Cells from the sham-treated control group underwent the same conditions, but the microwave generators were not energized. The supernatant temperature was measured before and after the microwave radiation using an optic fiber thermometer 3300 (Luxtron Corp.).

TEER, HRP Flux, and SEM Measurements

The BBB permeability was assessed by measuring the TEER across the cell monolayer. TEER represents the impedance required to pass through the barrier structure and is widely recognized as one of the most accurate and sensitive indicators of BBB integrity. A decrease in TEER reflects an increase in permeability and a loss of barrier function. The resistance value was multiplied by the surface area of the insert (1.12 cm^2) and expressed as ohms multiply by square centimeter. The TEER of each sample was corrected for background resistance without cells and reported as ohms multiply by square centimeter. The results were normalized to TEER measured before electromagnetic pulse (EMP) exposure and presented as absolute values.

Horseradish peroxidase (HRP, Sigma-Aldrich) transmissivity was measured in order to determine the in vitro BBB permeability to micromolecular materials. At 0, 6, 24, and 48 h after microwave exposure, the culture medium was replaced with DMEM without phenol red (Gibco) or serum. In order to maintain the culture supernatant level, 460 μl of medium containing 500 ng HRP was added into the insert, and 1,140 μl of medium was added into the well. A total of 50 μl of medium was collected from each well at different time points, which was replaced with 50 μl of fresh medium after each collection in order to maintain the liquid level on both sides. The collected samples were stored at 4 °C until processing, while 100 μl of peroxidase substrate containing tetramethyl benzidine and hydrogen peroxide was added to each sample and incubated for 10 min. The reaction was terminated by adding 50 μl of 2 M sulphuric acid. The optical density was measured at 450 nm, and the HRP transmissivity was assayed from the standard curve according to the following equation: $P_{\mathrm{HRP\%}}=[(C_{\mathrm{HRPo}}\times V_{\mathrm{o}}/C_{\mathrm{HRPi}}\times V_{\mathrm{i}})\times 100\ \%]$, where C_{HRPo} is the HRP concentration in the well, C_{HRPi} is the HRP concentration in the insert, V_{o} is the medium volume in the well, and V_{i} is the medium volume in the insert.

For scanning electron microscope (SEM) preparations, the co-culture cell model was fixed with 2.5 % glutaraldehyde in 0.12 M phosphate buffer (pH 7.5) overnight at 4 °C. After washing with phosphate buffer several times, the membranes of the culture inserts with the cells on both sides were removed from their support and placed into a 24-well chamber slide and then post-fixed in 1 % OsO_4 for 1 h at 4 °C. Following washing with distilled water, cells on the membrane were dehydrated in graded ethanol, critical point dried, and sputtered with 5 nm of gold layer for observation using a Hitachi S-3400-N field emission SEM.

RNA Extraction and qRT-PCR

Total RNA was extracted from ECV304 cells using TRIZOL reagent (Invitrogen) according to the manufacturer's protocol. Synthesis of cDNA and quantitative real-time PCR (qRT-PCR) reactions was performed using the PrimeScript TMRT reagent Kit (Takara). Primers were designed using the Primer 5.0 software. The forward and reverse primer sequences were as follows: occludin F, 5′-TCAAACCGAATCATTATGCA CCA-3′, occludin R, 5′-AGATGGCAATGCACATCACAA-3′ (189 bp); GAPDH F, 5′-GTGCTGAGTATGTCGTGGAG-3′, GAPDH R, 5′-CGGAGATGATGACCCTTTT-3′ (166 bp). The *GAPDH* gene was used as an internal standard. The $^{\Delta\Delta}$Ct method was used to transform Ct values into relative quantities with standard deviation. Changes were expressed as a percentage of the controls.

Immunoblotting, Immunoprecipitation, and Co-immunoprecipitation Assays

The ECV304 cells at 1, 6, 12, and 24 h after exposure were transferred to ice-cold buffer containing 20 mM EDTA, 0.1 mM sodium orthovanadate, 20 μg/ml aprotinin, 10 μg/ml leupeptin, and 0.1 mg/ml phenylmethylsulfonyl fluoride. Protein concentrations were determined using the BCA protein assay (Pierce).

Homogenates were mixed in the ratio of 3:2 with sample buffer containing 4 % sodium dodecyl sulfate (SDS), 250 mM Tris, 3 mM EDTA, 20 % glycerol, 5 % β-mercaptoethanol, and 0.05 % bromophenol blue (pH 8.0) at 95 °C for 10 min. For each condition, 25 μg of protein was loaded into each well on a 10 % SDS-polyacrylamide gel. After separation by electrophoresis, protein samples were electrotransferred onto a nitrocellulose membrane in transfer buffer (25 mM Tris/192 mM glycine/0.02 % SDS/20 % methanol) for 180 min at a constant current (26 mA). Additional protein binding sites on the nitrocellulose membrane were saturated by incubation in 10 mM PBS with 0.1 % Tween-20 (PBST, pH 7.4) containing 10 % dry milk powder for 1 h at room temperature. After a short wash with PBST, blots were incubated with antiserum to either occludin (1:250, polyclonal rabbit IgG, Invitrogen), ERK1/2 (1:500, polyclonal rabbit IgG, Invitrogen), p-ERK1/2 (1:600, polyclonal rabbit IgG, Cell Signal), p-c-Raf (1:500, polyclonal rabbit IgG, Cell Signal), p-MEK1/2 (1:450, polyclonal rabbit IgG, Cell Signal), VEGF (1:200, monoclonal mouse IgG, Santa Cruz), or Flk-1 (1:150, monoclonal mouse IgG, Santa Cruz) overnight at 4 °C. After rinsing three times with PBST, membranes were incubated with an anti-rabbit or anti-mouse HRP-conjugated secondary antibody (1:2,000, Zhongshanjinqiao) and HRP-conjugated monoclonal mouse IgG specific for GAPDH (1:10,000, Nanjingjiancheng) for 1 h at room temperature. Bands were developed on autoradiographic film by using an enhanced chemiluminescence kit (Pierce). The film signals were scanned using a high-resolution scanner, and the integral optical density of the scanned images was measured using a CMIAS-II image analyzer.

Three hundred micrograms of proteins were diluted in 250 μl of buffer containing 20 mM EDTA, 0.1 mM sodium orthovanadate, 20 μg/ml aprotinin, 10 μg/ml leupeptin, and 0.1 mg/ml phenylmethylsulfonyl fluoride. After incubating the solubilized homogenates with a phosphotyrosine (Invitrogen), p-ERK1/2, or occludin antibody conjugated to protein A-agarose (Santa Cruz) overnight at 4 °C, they were centrifuged at 2,500 rpm for 5 min at 4 °C. The supernatants were discarded and the pellets were washed with buffer (500 mM NaCl, 10 mM Tris, 2 mM EDTA, pH 7.5) four times before being centrifuged. The pellets were mixed in the proportion of 1:1 with 20 μl of the above buffer and 20 μl of sample buffer containing 4 % SDS, 250 mM Tris, 3 mM EDTA, 20 % glycerol, 5 % β-mercaptoethanol, and 0.05 % bromophenol blue (pH 8.0) and then heated at 100 °C for 5 min. After cooling the sample, it was centrifuged at 4,000 rpm for 10 min at 4 °C, and the supernatants were analyzed by SDS-polyacrylamide gel electrophoresis (PAGE). Proteins were resolved by 10 % SDS-PAGE and electrotransferred to 0.2-mm-thick nitrocellulose sheets for immunoblot analysis using occludin or p-ERK1/2 antibodies.

Immunohistochemistry

To determine the co-localization pattern of occludin and ZO-1, ECV304 cells were plated onto poly-D-lysine-coated glass cover slips in 6-well tissue culture plates at 6 h after microwave exposure. Sections or cover slips were washed in 0.1 M PBS and incubated with primary antibodies to ZO-1 (1:50, monoclonal mouse IgG, Invitrogen) and occludin (1:50, polyclonal rabbit IgG, Invitrogen) overnight, followed by incubation in 1 % BSA with secondary antibodies complex to either Alexa Fluor 568 or Alexa Fluor 488 (1:250, Invitrogen). Scans at different wavelengths were digitally merged and then sections were examined with a photomicroscope or laser scanning confocal microscope (LSCM: Radiance 2100™; Bio-Rad). Three areas of co-localization of occludin and ZO-1 were selected at random in each sample; co-localization of red and green signals was quantified using Image-Pro Plus [22].

Statistical Analysis

The results were expressed as means±standard error (SEM) and five subjects were used for each experiment. The differences between them were analyzed with one-way analysis of variance using SPSS v. 11.1 software and differences at the $P<0.05$ level were considered significant.

Results

Establishment of an In Vitro BBB Model and the BBB Permeability Increased Following Microwave Exposure

The epithelial-/endothelial-like human ECV304 cell line and primary astrocytes were used to establish an in vitro BBB model. ECV304 cells cultured in non-overlapping continuous monolayers displayed a cobblestone appearance and showed tightly apposed, elongated, polygonal, or short fusiform morphology and positive immunostaining for the endothelial marker, VIII factor (Fig. 1a, b). Following passage and differential adhesion, primary astrocytes were characterized by glial fibrillary acidic protein (GFAP) immunostaining (>95 %) and polygonal morphology with long cell processes resembling astrocytic endfeet, indicating a differentiated phenotype (Fig. 1c, d).

The ECV304 cells attached well to the collagen-coated filter surface of Snapwell cell culture inserts (Fig. 1e). As shown in Fig. 1f, there was no discernible morphological difference between the ECV304 cells growing in normal culture vessels and on the Snapwell cell culture inserts except for a tighter and more confluent arrangement. The number of ECV304 cells seeded was varied to obtain optimal confluence of the cells inside the insert, which was essential for a tight barrier. Therefore, the liquid level difference between the donor compartment and acceptor compartment was greater than 0.5 cm. After 4 h, 5-cm liquid medium levels were maintained in the in vitro BBB model, which showed that TJs were established.

The permeability of the cell monolayer to ions and low molecular weight molecules was assessed by measuring the TEER at 1–3 days before microwave exposure and 6–48 h after microwave exposure. At day 3 of co-culture, the BBB integrity was determined to be suitable by the obviously increased TEER values compared to that on day 1 ($P<0.01$) (Fig. 1g). Following exposure to microwave radiation, TEER

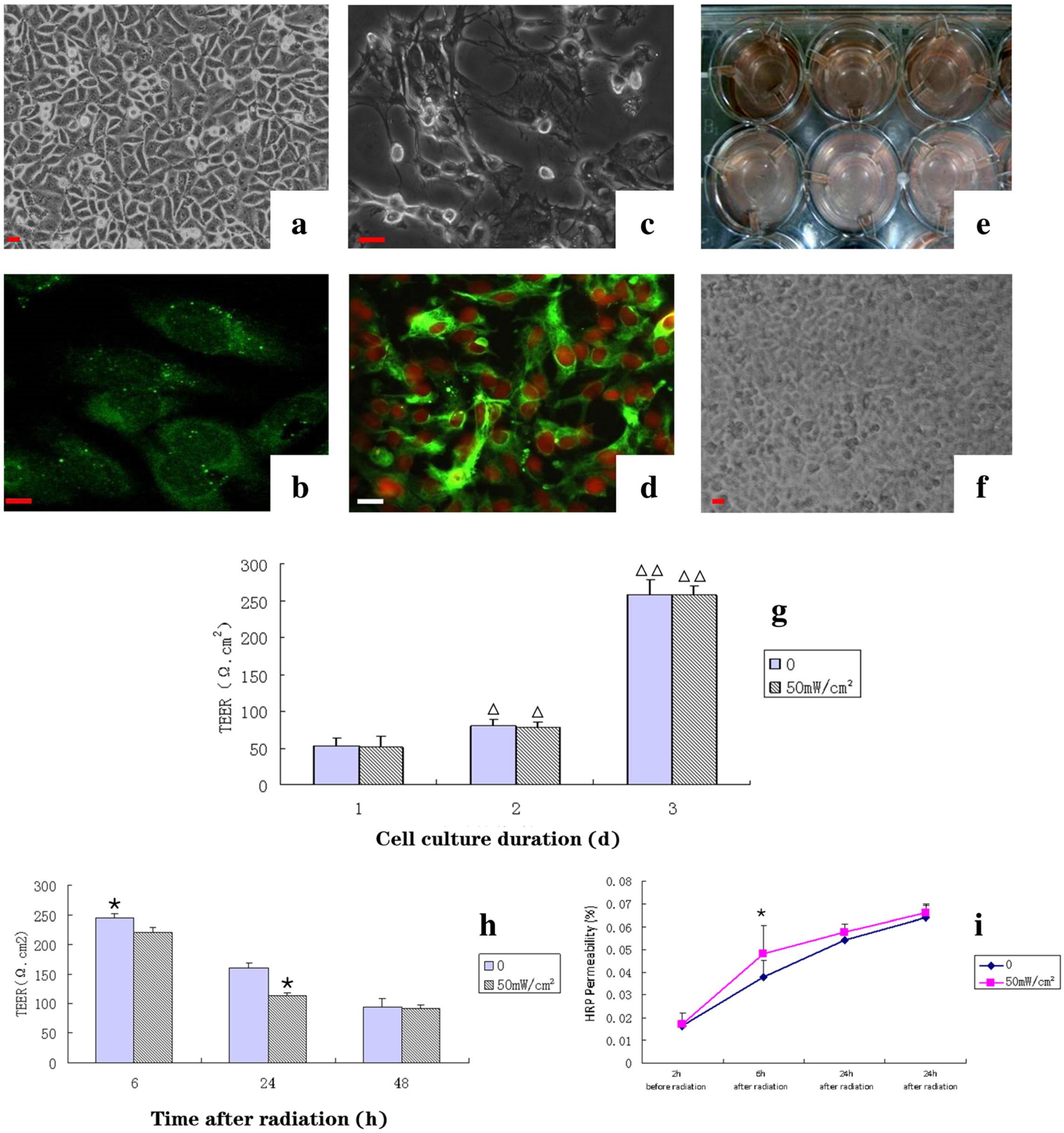

Fig. 1 Establishment of an in vitro BBB model and effect of microwave exposure on BBB permeability. **a** ECV304 cells grown in a monoculture model displayed a cobblestone appearance and tightly apposed, elongated, polygonal, or short fusiform morphology (IM *scale bar* 50 μm). **b** VIII factor was positively immunostained (green fluorescence) in the cytoplasm of ECV304 cells (LSCM *scale bar* 10 μm). **c** Primary astrocytes appeared polygonal with long cell processes resembling astrocytic endfeet at 17 days in culture and after three passages (IM *scale bar* 50 μm). **d** GFAP was strongly positively immunostained (green fluorescence) in the cytoplasm of primary astrocytes (LSCM *scale bar* 50 μm). **e**, **f** ECV304 cells and primary astrocytes were grown in a co-culture model in the obverse and reverse sides of Snapwell cell culture inserts. ECV304 cells were arranged tightly with astrocyte stimulation (IM *scale bar* 50 μm). **g** TEER values were increased on days 2 and 3 of co-culture compared to day 1 (n=5). **h** TEER values of the in vitro BBB model decreased at 24 h and returned to normal at 48 h following microwave exposure (50 mW/cm^2) (n=5). **i** HRP permeability increased at 6 h after microwave exposure (50 mW/cm^2) and then returned to normal levels. Each value represents the mean±SEM of samples (n=5). *P<0.05, **P<0.01, compared with corresponding sham-treated controls. $^{\Delta}P$<0.05, $^{\Delta\Delta}P$<0.01, compared with corresponding former time controls

values of the in vitro BBB model became unstable and decreased within 24 h compared to the sham-treated group (P<0.05). And at 48 h, there was no difference between the exposed group and the sham-treated group (Fig. 1h).

The permeability of the cell monolayer to low molecular weight molecules also was assessed by measuring the permeability coefficient of HRP at 2 h before and 6–48 h after microwave exposure. As shown in Fig. 1i, compared to the sham-treated group, the HRP permeability increased only at 6 h after microwave radiation ($P<0.05$).

Abnormal Expression of VEGF/Flk-1-ERK Pathway Components and Occludin in ECV304 Cells Following Microwave Radiation

Occludin messenger RNA (mRNA) in the ECV304 cells was detected by quantitative real-time PCR (qRT-PCR) at various times (1, 6, 12, and 24 h) following microwave radiation and was found to be decreased at the 6- and 12-h time points ($P<0.01$) (Fig. 2a) compared to the sham-treated group. Meanwhile, protein expression levels of VEGF-ERK-occludin signal transduction molecules in ECV304 cells were detected by Western blot at 1, 6, 12, and 24 h following microwave radiation at 50 mW/cm^2. Compared with the sham-treated controls, the immunoreactivity of VEGF increased at 1 and 12 h ($P<0.05$ or $P<0.01$) after radiation. In the same condition, Flk-1 increased at 1, 12, and 24 h ($P<0.05$ or $P<0.01$), p-c-Raf increased at 1, 6, and 24 h ($P<0.05$ or $P<0.01$), p-MEK increased at 6 h ($P<0.05$), p-ERK increased at 1 and 6 h ($P<0.05$ or $P<0.01$), and occludin decreased at 1, 6, and 12 h ($P<0.05$) (Fig. 2b, c). There was no change in expression of ERK between the exposed and sham-treated groups. These results indicated that microwave radiation partially activated the VEGF/Flk-1-ERK signal transduction but inhibited the expression of occludin.

The tyrosine phosphorylation of occludin in ECV304 cells was detected by immunoprecipitation at 1, 6, and 12 h following microwave radiation (50 mW/cm^2) and found to be increased at the 6 and 12 h time points ($P<0.01$) compared to the sham-treated group (Fig. 2d, e). The interactions between p-ERK and occludin in ECV304 cells were analyzed by co-immunoprecipitation at 1, 6, 12, and 24 h after exposure. When p-ERK was pulled down, the co-precipitated occludin was shown to be increased at 1, 6, and 12 h ($P<0.05$ or $P<0.01$) after radiation. When occludin was pulled down, the co-precipitated p-ERK was increased similarly at 1, 6, and 12 h ($P<0.05$ or $P<0.01$) after radiation compared with the sham-treated controls. Thus, microwave exposure enhanced the activity of occludin and the interaction between p-ERK and occludin in ECV304 cells.

Inhibition of Flk-1 or ERK Ameliorated the Damage to the Structure and Function of TJs by Microwave Radiation

An Flk-1 inhibitor (SU5416, 20 μmol/l) or MEK1/2 inhibitor (U0126, 10 μmol/l) was used at 30 min before microwave exposure (50 mW/cm^2) in the in vitro BBB model, and the effects of the intervention were detected at 1 and 6 h after radiation. The structure of ECV304 cells was observed by SEM at 6 h following microwave exposure. In the sham-treated group, there were rivet-like connections between the densely arranged cells, and the intercellular junctions were clear and continuous with a ridge-like or herringbone zipper pattern (Fig. 3a, b). At 6 h after radiation, the intercellular TJs were fractured and broadened (Fig. 3c, d). After SU5416 intervention, the structure of the TJs appeared only slightly broadened, and there were rivet-like connections in some areas (Fig. 3e, f). After U0126 treatment, the structure of TJs returned to normal levels (Fig. 3g, h). At 6 h after microwave radiation, the TEER values decreased, and the HRP permeability increased ($P<0.05$) in the ECV304/astrocyte co-culture model. After SU5416 or U0126 intervention, the TEER values increased, and the HRP permeability decreased ($P<0.05$ or $P<0.01$), compared to those in the exposed groups (Fig. 3i, j). Thus, inhibition of Flk-1 or MEK could ameliorate the damage to the structure and function of TJs by microwave radiation.

Fig. 2 Effect of microwave radiation on the expression of VEGF-ERK-occludin signal transduction molecules in ECV304 cells. **a** Abundance of occludin mRNA in ECV304 cells relative to the internal control GAPDH ($n=5$). **b** Representative Western blot results showing specific bands for VEGF, Flk-1, p-c-Raf, p-MEK1/2, ERK1/2, p-ERK1/2, occludin, and GAPDH in ECV304 cells. **c** Semi-quantitative levels of VEGF, Flk-1, p-c-Raf, p-MEK1/2, ERK1/2, p-ERK1/2, and occludin proteins are shown ($n=5$). **d** Results of immunoprecipitation and co-immunoprecipitation analyses showing specific bands for phosphorylated occludin and the interactions between p-ERK and occludin in ECV304 cells. **e** Semi-quantitative levels of phosphorylated occludin and interactions between p-ERK and occludin are shown ($n=5$). *$P<0.05$, **$P<0.01$, compared with sham-treated controls

Inhibition of Flk-1 or ERK Increased the Expression and Activity of Tight Junction Proteins in ECV304 Cells Following Microwave Radiation

The Flk-1 inhibitor (SU5416, 20 μmol/l) or MEK1/2 inhibitor (U0126, 10 μmol/l) was used at 30 min before microwave exposure in the ECV304 cells, and effects of the intervention were detected at 1 and 6 h after radiation. The increase of Flk-1 expression following the microwave exposure was inhibited by SU5416 treatment ($P<0.01$) (Fig. 4a). As shown in Figs. 4b–d and 5a, expression levels of p-c-Raf, p-MEK1/2, and p-ERK were inhibited; the expression and interaction of occludin with ZO-1 were accelerated; and the phosphorylation and interaction of occludin with p-ERK were down-regulated ($P<0.05$ or $P<0.01$) after SU5416 treatment. Likewise, immunoreactivities of p-MEK1/2 and p-ERK were inhibited, the expression and interaction of occludin with ZO-1 were accelerated, and the phosphorylation and interaction of occludin

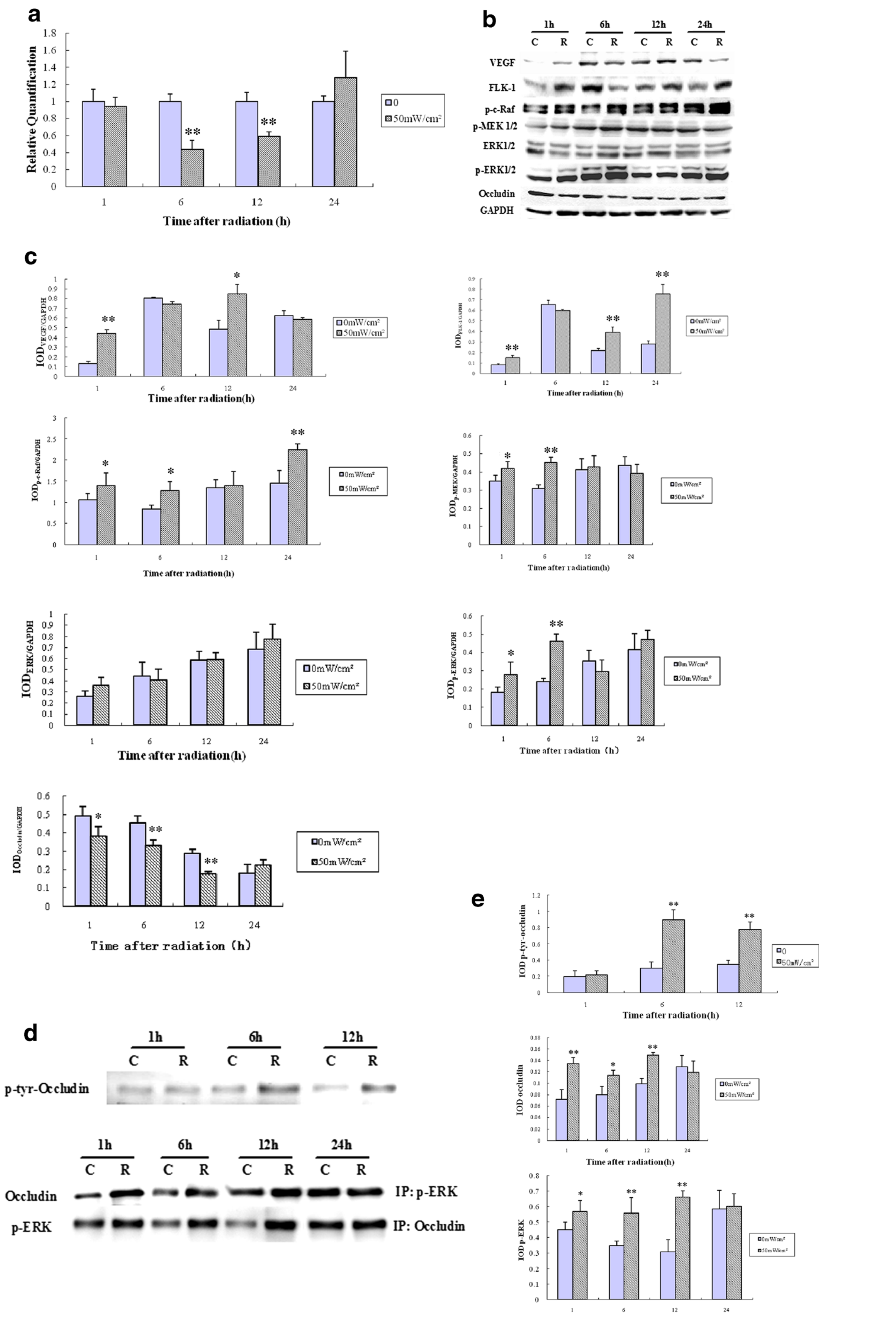
a
Relative Quantification
Time after radiation (h)
0
50mW/cm²
b
1h
6h
12h
24h
C
R
VEGF
FLK-1
p-c-Raf
p-MEK 1/2
ERK1/2
p-ERK1/2
Occludin
GAPDH
c
Time after radiation(h)
0mW/cm²
50mW/cm²
d
p-tyr-Occludin
Occludin
p-ERK
IP: p-ERK
IP: Occludin
e
IOD p-tyr-occludin
IOD occludin
IOD p-ERK

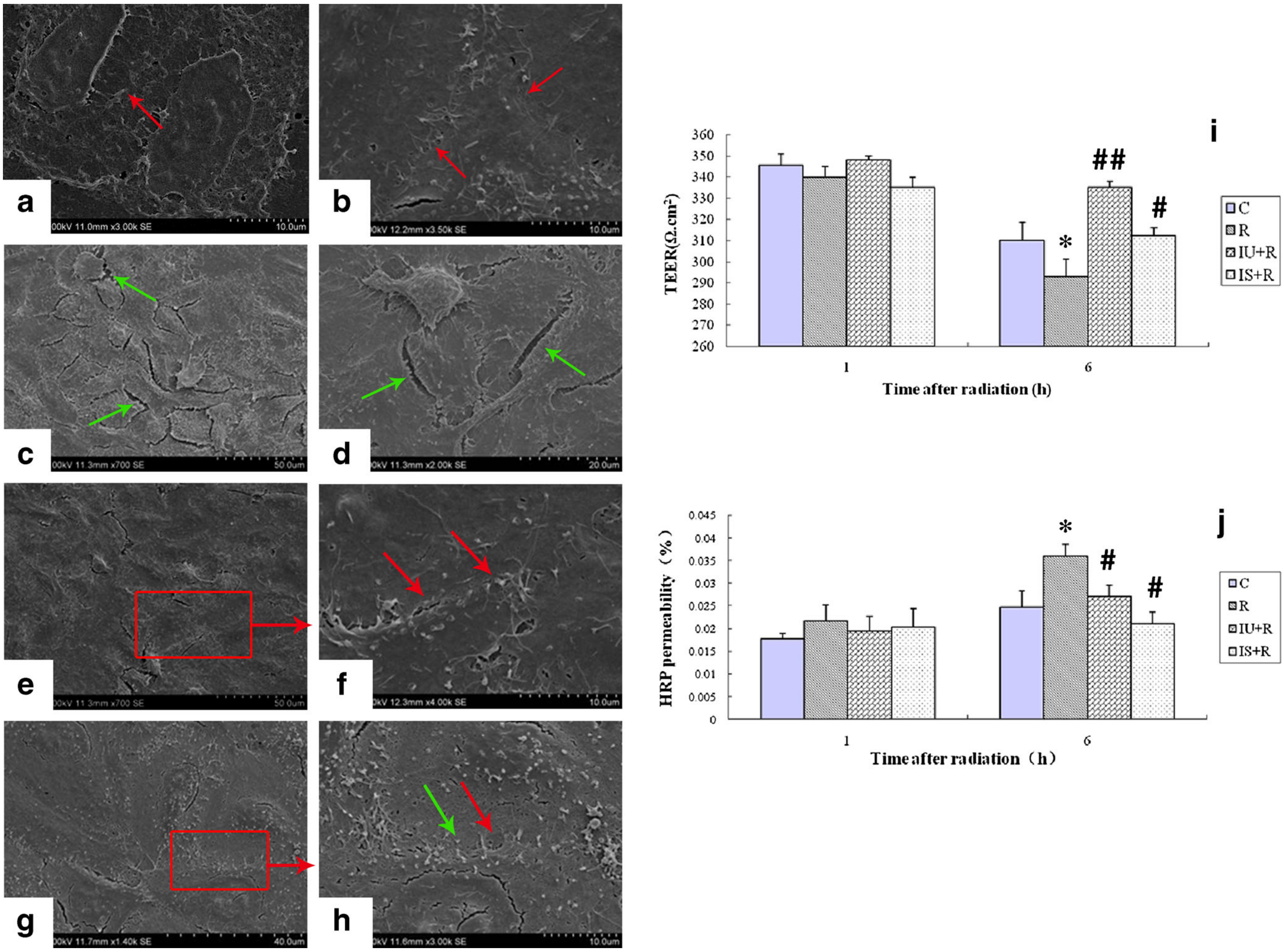

Fig. 3 Effect of Flk-1 or ERK on the structure and function of BBB after microwave exposure (SEM). **a**, **b** In the sham-treated group, intercellular junctions were clear and continuous with a ridge or herringbone zipper pattern (*red arrow*) (*scale bar* 10 μm). **c**, **d** At 6 h after microwave radiation (50 mW/cm^2), the intercellular TJs became fractured and broadened (*green arrow*) (**c** *scale bar* 50 μm; **d** *scale bar* 20 μm). **e**, **f** After SU5416 intervention and microwave radiation (50 mW/cm^2), the structure of TJs was slightly broadened (*green arrow*), with rivet-like connections in certain parts (*red arrow*) (**e** *scale bar* 50 μm; **f** *scale bar* 10 μm). **g**, **h** After U0126 intervention and microwave radiation (50 mW/cm^2), the rivet-like connections were arranged densely, and the intercellular junctions were clear and continuous with ridges (*red arrow*) (**g** *scale bar* 40 μm; **h** *scale bar* 10 μm). **i** TEER values were decreased in ECV304/astrocyte co-culture models at 6 h after microwave radiation. After SU5416 or U0126 intervention, the TEER values were increased compared to the exposed groups (n=5). **j** HRP permeability was increased at 6 h after microwave radiation in the ECV304/astrocyte co-culture model (n=5). After SU5416 or U0126 intervention, the HRP permeability was decreased compared to the exposed groups. *P<0.05, **P<0.01, compared with corresponding sham-treated controls. $^{\#}P$<0.05, $^{\#\#}P$<0.01, compared with the exposed groups

with p-ERK were down-regulated (P<0.05 or P<0.01) after U0126 treatment. The co-localization of occludin and ZO-1 was detected by immunofluorescence at 6 h after radiation as shown in Fig. 5b–n. In the sham-treated group, expression of occludin and ZO-1 was overlapped in the ECV304 cell membrane (Fig. 5b–d). After microwave exposure, occludin and ZO-1 expression levels decreased, and their signals were discontiguous and mainly not co-localized (P<0.01) (Fig. 5e–g). After treatment by SU5416 or U0126, the co-expression of occludin and ZO-1 increased (P<0.05 or P<0.01), especially after U0126 intervention (Fig. 5h–m). Thus, inhibition by SU5416 or U0126 muted the increase in expression of ERK signal transduction molecules, while

Fig. 4 Effect of Flk-1 or ERK on the expression and activity of TJ ▶ proteins in ECV304 cells following microwave radiation. **a** Representative Western blot analysis detecting specific bands for Flk-1 and GAPDH (upper). Semi-quantitative levels of Flk-1 after SU5416 intervention (lower, n=5). **b** Representative Western blot results showing specific bands for p-c-Raf, p-MEK1/2, ERK1/2, p-ERK1/2, occludin, and GAPDH after SU5416 or U0126 intervention in ECV304 cells. **c** Semi-quantitative levels of p-c-Raf, p-MEK1/2, ERK1/2, p-ERK1/2, and occludin proteins after SU5416 or U0126 intervention are shown (n=5). **d** Results of immunoprecipitation and co-immunoprecipitation analysis showing specific bands for phosphorylated occludin and interactions between p-ERK and occludin after SU5416 or U0126 intervention in ECV304 cells (*upper left*). Semi-quantitative levels of phosphorylated occludin and interactions between p-ERK and occludin after SU5416 or U0126 intervention are shown (*upper right* and *lower*, n=5). *P<0.05, **P<0.01, compared with corresponding sham-treated controls. $^{\#}P$<0.01, $^{\#\#}P$<0.05, compared with the exposed groups

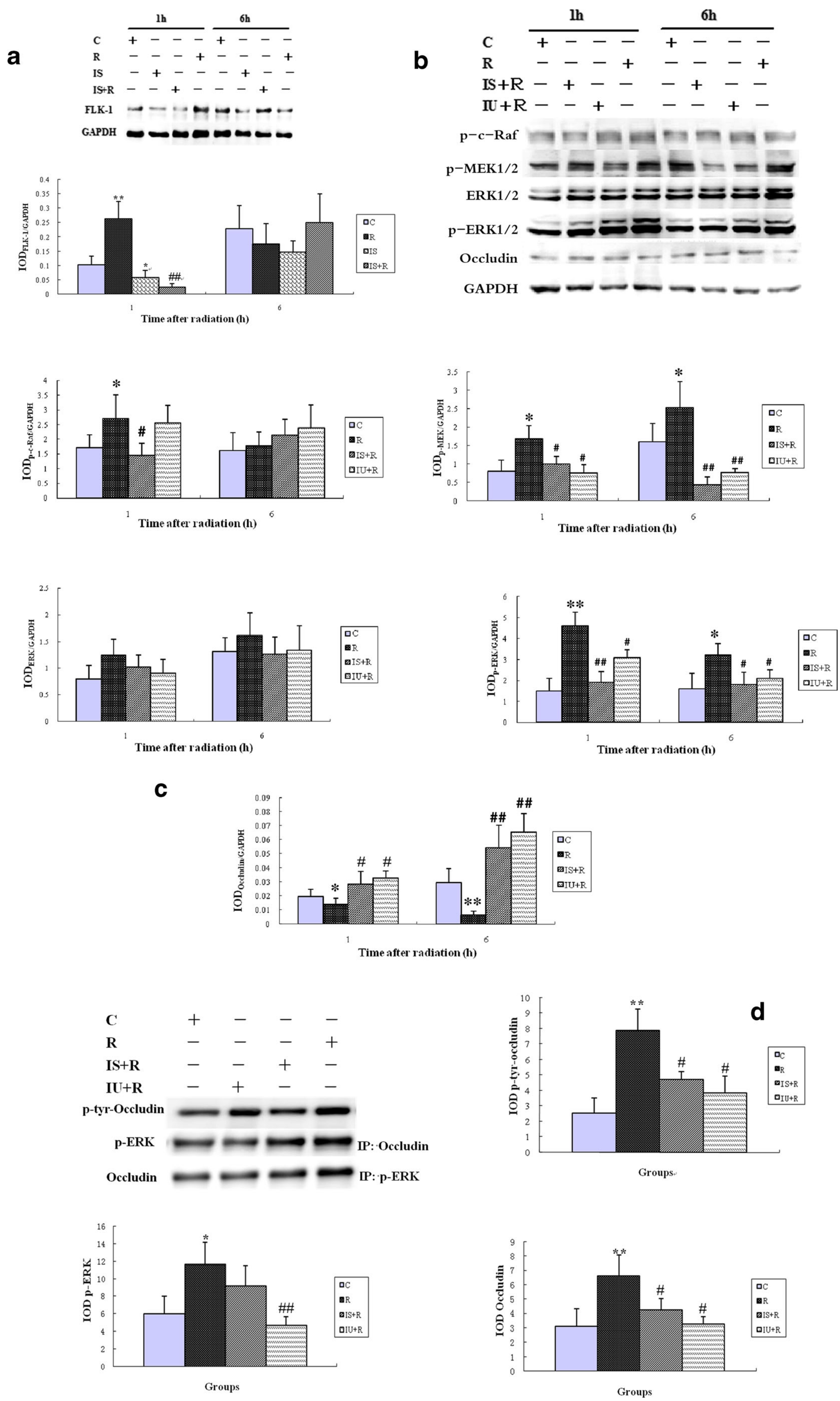
a
1h
6h
C
R
IS
IS+R
FLK-1
GAPDH
IOD FLK-1/GAPDH
Time after radiation (h)
b
p-c-Raf
p-MEK1/2
ERK1/2
p-ERK1/2
Occludin
GAPDH
IU+R
IOD p-c-Raf/GAPDH
IOD p-MEK/GAPDH
IOD ERK/GAPDH
IOD p-ERK/GAPDH
c
IOD Occludin/GAPDH
p-tyr-Occludin
p-ERK
IP: Occludin
IP: p-ERK
d
IOD p-tyr-occludin
IOD p-ERK
IOD Occludin
Groups

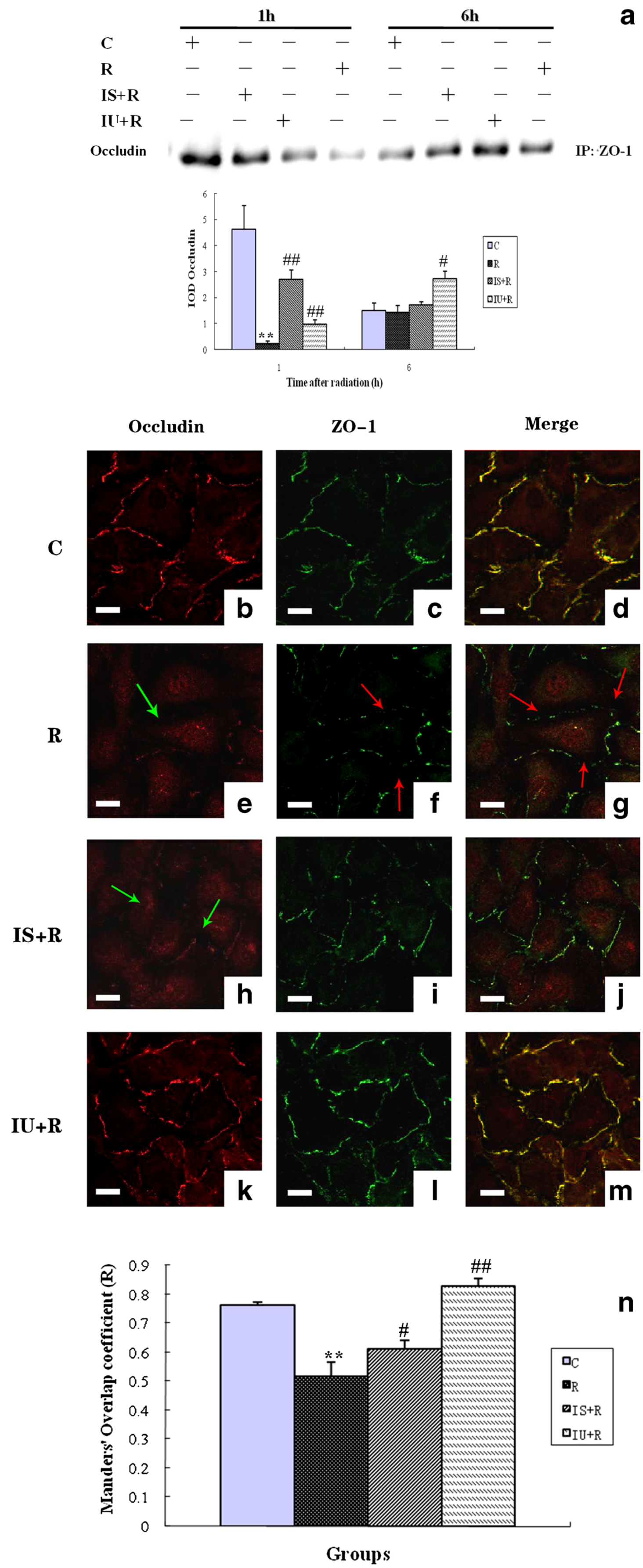

Fig. 5 Effect of Flk-1 or ERK on the interaction and co-localization of occludin and ZO-1 in ECV304 cells following microwave radiation (LSCM *scale bar* 10 μm). **a** Representative co-immunoprecipitation analysis showing specific bands for the interactions between occludin and ZO-1 after SU5416 or U0126 intervention (*upper*). Semi-quantitative levels of co-immunoprecipitation analysis for the interactions between occludin and ZO-1 after SU5416 or U0126 intervention (*lower*, n=5). **b–d** In the sham-treated group, occludin and ZO-1 signals were overlapped in the ECV304 cell membrane. **e–g** Occludin and ZO-1 were distributed as dots or discontiguous signals (*green* or *red arrow*) in the ECV304 cell membrane after microwave exposure. **h–j** After SU5416 intervention and microwave radiation, the expression of occludin was discontiguous (*green arrow*) and that of ZO-1 was contiguous. **k–m** After U0126 intervention and microwave radiation, the signals of occludin and ZO-1 were overlapped. **n** Semi-quantitative levels of co-localization of occludin and ZO-1 after SU5416 or U0126 intervention (n=3). *P<0.05, **P<0.01, compared with corresponding sham-treated controls. $^{\#}P$<0.01, $^{\#\#}P$<0.05, compared with the exposed groups

accelerated the expression and activity of occludin, as well as the interactions of occludin with p-ERK and ZO-1 following microwave radiation.

Discussion

The BBB prevents the free passage of various molecules from the blood into the CNS. Previous studies have shown that exposure to microwaves can increase the permeability of the BBB to small molecules such as sucrose, Evans-Blue dye, lanthanum nitrate, and albumin [21, 23, 24]. Although these studies have focused mainly on thermal effects, microwaves also exert non-thermal effects on the BBB. In our study, the microwave exposure to BBB was non-thermal since no temperature change occurred in the culture medium. However, there were still some negative effects and found that the BBB permeability did not change after exposure to low-power 2,450 MHz and 1,439 Hz continuous waves, 1.8 GHz and 915 MHz pulses and continuous waves [25–28].

In the current study, we established an in vitro BBB model using the epithelial/endothelial-like human ECV304 cell line and primary astrocytes. The BBB integrity was determined to be suitable for subsequent experiments, as shown by the increased TEER values and maintenance of culture medium levels in the transwells at 5 cm. Based on the preliminary work (data was not shown), we used the microwave dosage, 50 mW/cm^2 for 5 min at 2.856 GHz, in the mechanism studies which could induce the ECV304 cell injury but not elevated temperature in the cell medium. After microwave exposure at 50 mW/cm^2, the intercellular TJs of ECV304 cells were fractured and broadened, while TEER values of the in vitro BBB model tended to decrease and the HRP permeability increased. These results indicated that the structure of the BBB was damaged and the permeability of ions and low-molecular-weight molecules was increased. Likewise, Zhou et al. [29] established an in vitro BBB model by co-culturing brain microvascular endothelial cells and astroglial cells isolated from rat brains which were exposed to electromagnetic pulses at 100 and 400 kV/m. They found that the TEER level was lower and the HRP permeability of the BBB model was increased after the exposure. While the increased permeability may help therapeutic drugs cross the BBB [30], it also can allow deleterious molecules into the brain and aggravate the injury induced by microwave exposure [31]. Although changes induced by microwaves are transient, the mechanism by which they induce BBB injury requires further study.

Occludin and the claudin family proteins are the most important membranous components of the BBB TJs that have been identified. Occludin may play an important role in the regulation of tight junction integrity rather than in the assembly of tight junction [32, 33]. ZO-1 serves as a critical linker between peri-junctional actin and the TJ proteins occludin and claudins [34–37]. There is an association between TJ morphology and the expression of TJ proteins in endothelial cells of the BBB [38, 39], as well as between the expression of these proteins and the manifestation of specific characteristics (low permeability and high TEER) of the barrier in the cerebral microvasculature [7, 40–44]. Electromagnetic pulses (EMP) were found to induce the decrease in gene and protein expression of occludin and ZO-1 in homogenates of both the cerebral cortex homogenate and cerebral cortex microvessels of rats and alter ZO-1 localization; however, they did not change the distribution of occludin [45]. Other studies showed that permeation of transporter substrates at the BBB as well as the localization and integrity of the TJ proteins occludin and ZO-1 were not affected after EMP exposure [23]. In our previous study, we found that the mRNA and protein expression of occludin and ZO-1 decreased, while the level of p-Tyr-occludin increased in the hippocampus and cerebral cortex after microwave radiation [46]. In this study, we detected the expression of TJ proteins in an in vitro BBB model and found decreased occludin mRNA and protein along with increased Tyr phosphorylation of occludin in ECV304 cells following microwave radiation. Other studies have indicated that occludin is highly phosphorylated on Ser and Thr residues, while Tyr phosphorylation is kept at minimum in the intact epithelium. The Tyr phosphorylation of TJ and adherent junction proteins may play a role in the disruption of these junctional complexes, and the Tyr phosphorylation of occludin may attenuate its interaction with ZO-1, leading to a disruption of TJs [32, 33, 47]. Thus, after microwave radiation, the increased expression and decreased Tyr phosphorylation of occludin can both aggravate the damage to the structure and function of TJs.

Many types of extracellular stimuli can initiate intracellular signaling pathways and modulate the expression of TJ proteins. As a cytokine involved in the inflammatory response, VEGF may contribute to the disruption of the BBB and facilitate the progression of secondary brain damage. This factor induces Tyr kinase receptor phosphorylation, as well as internalization and cleavage of VE-cadherin, which can cause dismantling of adherent junctions and an increase in vascular permeability. VEGF-A, the prototype VEGF ligand, binds and activates two Tyr kinase receptors: VEGFR-1 (Flt-1) and VEGFR-2 (KDR/Flk-1). Endothelial adherent junctions are well known to be a downstream target of Flk-1 signaling, and it has been suggested that Tyr phosphorylation of its components may be involved in the loosening of cell–cell contacts in established vessels to modulate transendothelial permeability. Additionally, the overexpression of VEGF and its receptor Flk-1 corresponds temporally and spatially with the disruption of the BBB integrity [13, 48–51]. In our previous study [52], we found that the VEGF and Flk-1 expression in the cytoplasm of neurons and cell membrane of endothelial cells in the hippocampus become augmented at 7 days and peaked at 14 days or 1 month after microwave exposure at 5 or 10 mW/cm^2, respectively. Those results indicated that VEGF and Flk-1 may participate in the structural and functional damage of the hippocampus, but the role of VEGF in the permeability of BBB still needed to be examined in further detail.

In the in vitro BBB model established in the current study, we found that, among the VEGF-ERK-occludin signal transduction molecules detected, VEGF, Flk-1 p-c-Raf, p-MEK, and p-ERK were all increased following microwave exposure (50 mW/cm^2). These observations showed that microwave exposure might partially activate VEGF/Flk-1-ERK signaling transduction. Basuroy et al. [53] used glutathione S-transferase (GST) pull-down assays and pairwise binding studies with ERK recombinant proteins to determine that the C-terminal tail of occludin binds to p-ERK in Caco-2 cell extracts and that ERK1 directly interacts with the C-terminal tail of occludin. To investigate the regulatory role of ERK, we first performed co-immunoprecipitation experiments and determined that the interaction between p-ERK and occludin was enhanced after microwave exposure. Subsequently, by using inhibitors of Flk-1 (SU5416) and MEK1/2 (U0126) after microwave exposure, expression levels of p-c-Raf, p-MEK1/2, and p-ERK were found to be inhibited. Meanwhile, the expression of occludin as well as its interaction and co-localization with ZO-1 were enhanced, but its phosphorylation and interaction with p-ERK were down-regulated. Compared to the exposed groups, the cells of groups treated with SU5416 or U0126 after radiation showed repaired TJs structure, increased TEER values, and decreased HRP permeability. Therefore, the inhibition of Flk-1 or p-ERK following microwave radiation can induce the expression and Tyr dephosphorylation of occludin as well as its interaction with ZO-1, which may facilitate the repair of BBB injury. In conclusion, microwave radiation can activate VEGF-ERK signal transduction, which accelerates the Tyr phosphorylation of occludin but partially inhibits occludin expression and interaction with ZO-1, further aggravating the structural and functional damage to the BBB (Fig. 6).

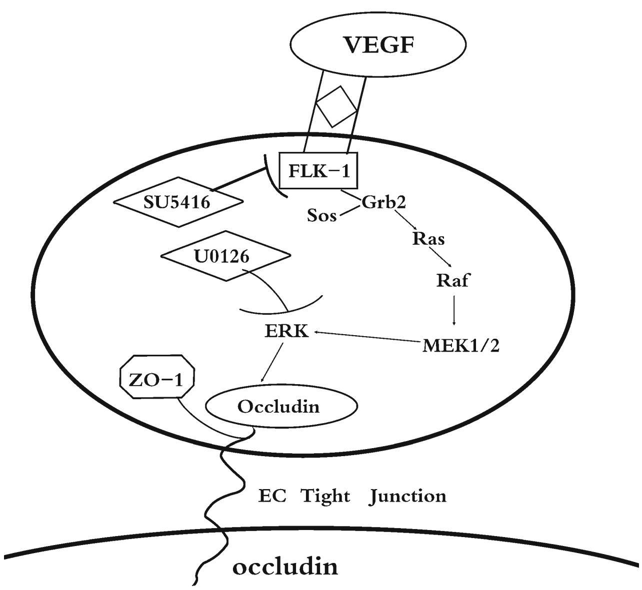

Fig. 6 The role of VEGF/Flk-1-Raf/MEK/ERK pathway on occludin

Acknowledgments This work was supported by the National Natural Science Foundation of China (81172620 and 81372926) and Beijing Natural Science Foundation (7122127). We are grateful to Sa Zhang and Kai Wang of the National Center of Biomedical Analysis for their kind help with electron microscopy and laser scanning confocal microscopy, Associate Professor Yue-Feng Yang and Guang-Xing Bian of Beijing Institute of Radiation Medicine for in vitro BBB models.

Authors' Contributions The work presented here was carried out in collaboration between all authors. Rui-Yun Peng and Xiang-Jun Hu conceived the project. Li-Feng Wang and Xiang Li performed the experiments. Shui-Ming Wang and Ya-Bing Gao conceived the study and participated in the design of the study. Ji Dong, Li Zhao, and Bin-Wei Yao participated in sample collection. Xin-Ping Xu performed the quantitative analysis. Gong-Min Chang helped to analyze the data and performed the statistical analysis. Hong-Mei Zhou was responsible for microwave radiation.

Conflict of Interest The author(s) declare that they have no competing interests.

References

1. Kesari KK, Kumar S, Behari J (2012) Pathophysiology of microwave radiation: effect on rat brain. Appl Biochem Biotechnol 166:379–388
2. Mortazavi SM, Mahbudi A, Atefi M, Bagheri S, Bahaedini N et al (2011) An old issue and a new look: electromagnetic hypersensitivity caused by radiations emitted by GSM mobile phones. Technol Health Care 19:435–443
3. Del Vecchio G, Giuliani A, Fernandez M, Mesirca P, Bersani F et al (2009) Effect of radiofrequency electromagnetic field exposure on in vitro models of neurodegenerative disease. Bioelectromagnetics 30:564–572
4. Kuo YC, Lu CH (2011) Effect of human astrocytes on the characteristics of human brain-microvascular endothelial cells in the blood-brain barrier. Colloids Surf B Biointerfaces 86:225–231
5. Thal SC, Luh C, Schaible EV, Timaru-Kast R, Hedrich J et al (2012) Volatile anesthetics influence blood-brain barrier integrity by modulation of tight junction protein expression in traumatic brain injury. PLoS One 7:e50752
6. Liebner S, Kniesel U, Kalbacher H, Wolburg H (2000) Correlation of tight junction morphology with the expression of tight junction proteins in blood-brain barrier endothelial cells. Eur J Cell Biol 79: 707–717
7. Hawkins BT, Davis TP (2005) The blood-brain barrier/neurovascular unit in health and disease. Pharmacol Rev 57:173–185
8. Wolburg H, Lippoldt A (2002) Tight junctions of the blood-brain barrier: development, composition and regulation. Vascul Pharmacol 38:323–337
9. Balbuena P, Li W, Ehrich M (2011) Assessments of tight junction proteins occludin, claudin 5 and scaffold proteins ZO1 and ZO2 in endothelial cells of the rat blood-brain barrier: cellular responses to

neurotoxicants malathion and lead acetate. Neurotoxicology 32:58–67
10. Lafuente JV, Argandona EG, Mitre B (2006) VEGFR-2 expression in brain injury: its distribution related to brain-blood barrier markers. J Neural Transm 113:487–496
11. Do B (2010) Vascular endothelial growth factors and vascular permeability. Cardiovasc Res 87:262–271
12. Wang WDW, Borchardt RT (2001) VEGF increases BMEC monolayer permeability by affecting occludin expression and tight junction assembly. Am J Physiol Heart Circ Physiol 280: H434–H440
13. Kaya D, Gursoy-Ozdemir Y, Yemisci M, Tuncer N, Aktan S et al (2005) VEGF protects brain against focal ischemia without increasing blood-brain permeability when administered intracerebroventricularly. J Cereb Blood Flow Metab 25:1111–1118
14. Storkebaum E, Lambrechts D, Carmeliet P (2004) VEGF: once regarded as a specific angiogenic factor, now implicated in neuroprotection. Bioessays 26:943–954
15. Wachtel M, Frei K, Ehler E, Bauer C, Gassmann M et al (2002) Extracellular signal-regulated protein kinase activation during reoxygenation is required to restore ischaemia-induced endothelial barrier failure. Biochem J 367:873–879
16. Gonzalez-Mariscal L, Tapia R, Chamorro D (2008) Crosstalk of tight junction components with signaling pathways. Biochim Biophys Acta Biomembr 1778:729–756
17. Ning L, Kunnimalaiyaan M, Chen H (2008) Regulation of cell-cell contact molecules and the metastatic phenotype of medullary thyroid carcinoma by the Raf-1/MEK/ERK pathway. Surgery 144:920–924, discussion 924–925
18. Salford LG, Brun A, Sturesson K, Eberhardt JL, Persson BR (1994) Permeability of the blood-brain barrier induced by 915 MHz electromagnetic radiation, continuous wave and modulated at 8, 16, 50, and 200 Hz. Microsc Res Tech 27:535–542
19. Schirmacher A, Winters S, Fischer S, Goeke J, Galla HJ et al (2000) Electromagnetic fields (1.8 GHz) increase the permeability to sucrose of the blood-brain barrier in vitro. Bioelectromagnetics 21:338–345
20. Williams WM, Del Cerro M, Michaelson SM (1984) Effect of 2450 MHz microwave energy on the blood-brain barrier to hydrophilic molecules. B. Effect on the permeability to HRP. Brain Res 319:171–181
21. Zhang YM, Zhou Y, Qiu LB, Ding GR, Pang XF (2012) Altered expression of matrix metalloproteinases and tight junction proteins in rats following PEMF-induced BBB permeability change. Biomed Environ Sci 25:197–202
22. Vadim Zinchuka OG-Z (2009) Recent advances in quantitative colocalization analysis: focus on neuroscience. Prog Histochem Cytochem 44:125–172
23. Ding GR, Qiu LB, Wang XW, Li KC, Zhou YC et al (2010) EMP-induced alterations of tight junction protein expression and disruption of the blood-brain barrier. Toxicol Lett 196:154–160
24. Nittby H, Brun A, Eberhardt J, Malmgren L, Persson BR et al (2009) Increased blood-brain barrier permeability in mammalian brain 7 days after exposure to the radiation from a GSM-900 mobile phone. Pathophysiology 16:103–112
25. Franke H, Streckert J, Bitz A, Goeke J, Hansen V et al (2005) Effects of Universal Mobile Telecommunications System (UMTS) electromagnetic fields on the blood-brain barrier in vitro. Radiat Res 164: 258–269
26. Franke H, Ringelstein EB, Stogbauer F (2005) Electromagnetic fields (GSM 1800) do not alter blood-brain barrier permeability to sucrose in models in vitro with high barrier tightness. Bioelectromagnetics 26:529–535
27. Kuribayashi M, Wang J, Fujiwara O, Doi Y, Nabae K et al (2005) Lack of effects of 1439 MHz electromagnetic near field exposure on the blood-brain barrier in immature and young rats. Bioelectromagnetics 26:578–588
28. McQuade JM, Merritt JH, Miller SA, Scholin T, Cook MC et al (2009) Radiofrequency-radiation exposure does not induce detectable leakage of albumin across the blood-brain barrier. Radiat Res 171:615–621
29. Zhou JX, Ding GR, Zhang J, Zhou YC, Zhang YJ et al (2013) Detrimental effect of electromagnetic pulse exposure on permeability of in vitro blood-brain-barrier model. Biomed Environ Sci 26:128–137
30. Kuo YC, Lu CH (2012) Modulation of efflux proteins by electromagnetic field for delivering azidothymidine and saquinavir into the brain. Colloids Surf B Biointerfaces 91: 291–295
31. Stam R (2010) Electromagnetic fields and the blood-brain barrier. Brain Res Rev 65:80–97
32. Murakami T, Felinski EA, Antonetti DA (2009) Occludin phosphorylation and ubiquitination regulate tight junction trafficking and vascular endothelial growth factor-induced permeability. J Biol Chem 284:21036–21046
33. Rao R (2009) Occludin phosphorylation in regulation of epithelial tight junctions. Ann N Y Acad Sci 1165:62–68
34. Aschner M, Fitsanakis VA, dos Santos AP, Olivi L, Bressler JP (2006) Blood-brain barrier and cell-cell interactions: methods for establishing in vitro models of the blood-brain barrier and transport measurements. Methods Mol Biol 341:1–15
35. Shah KK, Yang L, Abbruscato TJ (2012) In vitro models of the blood-brain barrier. Methods Mol Biol 814:431–449
36. Wilhelm I, Fazakas C, Krizbai IA (2011) In vitro models of the blood-brain barrier. Acta Neurobiol Exp (Wars) 71:113–128
37. Musch MW, Walsh-Reitz MM, Chang EB (2006) Roles of ZO-1, occludin, and actin in oxidant-induced barrier disruption. Am J Physiol Gastrointest Liver Physiol 290:G222–G231
38. Helms HC, Waagepetersen HS, Nielsen CU, Brodin B (2010) Paracellular tightness and claudin-5 expression is increased in the BCEC/astrocyte blood-brain barrier model by increasing media buffer capacity during growth. AAPS J 12:759–770
39. Liebner S, Fischmann A, Rascher G, Duffner F, Grote EH et al (2000) Claudin-1 and claudin-5 expression and tight junction morphology are altered in blood vessels of human glioblastoma multiforme. Acta Neuropathol 100:323–331
40. Wuest DM, Wing AM, Lee KH (2013) Membrane configuration optimization for a murine in vitro blood-brain barrier model. J Neurosci Methods 212:211–221
41. Bohara M, Kambe Y, Nagayama T, Tokimura H, Arita K et al (2014) C-type natriuretic peptide modulates permeability of the blood-brain barrier. J Cereb Blood Flow Metab
42. Cioni C, Turlizzi E, Zanelli U, Oliveri G, Annunziata P (2012) Expression of tight junction and drug efflux transporter proteins in an in vitro model of human blood-brain barrier. Front Psychiatry 3:47
43. Zehendner CM, Librizzi L, Hedrich J, Bauer NM, Angamo EA et al (2013) Moderate hypoxia followed by reoxygenation results in blood-brain barrier breakdown via oxidative stress-dependent tight-junction protein disruption. PLoS One 8: e82823
44. Zhu H, Wang Z, Xing Y, Gao Y, Ma T et al (2012) Baicalin reduces the permeability of the blood-brain barrier during hypoxia in vitro by increasing the expression of tight junction proteins in brain microvascular endothelial cells. J Ethnopharmacol 141:714–720
45. Qiu LB, Ding GR, Zhang YM, Zhou Y, Wang XW et al (2009) Effects of electromagnetic pulse on blood-brain barrier permeability and tight junction proteins in rats. Zhonghua Lao Dong Wei Sheng Zhi Ye Bing Za Zhi 27:539–543
46. Li X, Peng R-Y, Hu X, Wang S, Gao Y, Wang L et al (2011) Changes and significance of occludin expression in rats with blood-brain

barrier injury induced by microwave radiation. Med J Chin People's Liberation Army 36:765–769
47. DeMaio L, Chang YS, Gardner TW, Tarbell JM, Antonetti DA (2001) Shear stress regulates occludin content and phosphorylation. Am J Physiol Heart Circ Physiol 281:H105–H113
48. Salmeri M, Motta C, Anfuso CD, Amodeo A, Scalia M et al (2013) VEGF receptor-1 involvement in pericyte loss induced by *Escherichia coli* in an in vitro model of blood brain barrier. Cell Microbiol 15:1367–1384
49. Dejana E, Orsenigo F, Lampugnani MG (2008) The role of adherens junctions and VE-cadherin in the control of vascular permeability. J Cell Sci 121:2115–2122
50. Davis B, Tang J, Zhang L, Mu D, Jiang X et al (2010) Role of vasodilator stimulated phosphoprotein in VEGF induced blood-brain barrier permeability in endothelial cell monolayers. Int J Dev Neurosci 28:423–428
51. Mendonca MC, Soares ES, Stavale LM, Raposo C, Coope A et al (2013) Expression of VEGF and Flk-1 and Flt-1 receptors during blood-brain barrier (BBB) Impairment following *Phoneutria nigriventer* spider venom exposure. Toxins (Basel) 5:2572–2588
52. Li X, Peng R-Y, Hu XJ, Wang SM, Gao Y, Wang L, Zhao L, Dong J et al (2010) Effects of microwave exposure on VEGF and FLK-1 of hippocampus in the rats. Chin J Stereology Image Anal 4:017
53. Basuroy S, Seth A, Elias B, Naren AP, Rao R (2006) MAPK interacts with occludin and mediates EGF-induced prevention of tight junction disruption by hydrogen peroxide. Biochem J 393:69–77